Thin-Film Assisted Laser Transfer and Bonding (TFA-LTAB) for the Fabrication of Micro-LED Displays

(article starts on next page)

Thin-Film Assisted Laser Transfer and Bonding (TFA-LTAB) for the Fabrication of Micro-LED Displays

Taifu Lang, Xin Lin, Xiaowei Huang, Yujie Xie, Shuangjia Bai, Yijian Zhou, Shuaishuai Wang, Yu Lu, Xuehuang Tang, Chang Lin, Zhonghang Huang, Kaixin Zhang, Qun Yan, and Jie Sun*

Micro-Light Emitting Diodes (Micro-LEDs) are key components in the field of next-generation display technologies. In the process of making Micro-LED displays, millions of chips need to be transferred to the driver substrate using mass transfer technology. Conventional transfer techniques, such as stamp transfer, present challenges in terms of processing efficiency and applicability due to the need for pre-prepared tethered structures and fixed chip pitch. To overcome these limitations, the t hin-film-assisted laser transfer and bonding (TFA-LTAB) technology is proposed. This technique is able to efficiently and accurately transfer Micro-LEDs from the source substrate to the driver substrate with arbitrary pitch through thin-film assistance, and electrically connects the chips through flip-chip bonding technology, which significantly improves the efficiency and reliability of the transfer and joining. The TFA-LTAB method proposed in this study integrates laser transfer and flip-chip bonding techniques. Through the TFA-LTAB process, these Micro-LEDs cultured on sapphire substrates are precisely assembled onto transparent low-temperature polycrystalline silicon thin-film transistors (LTPS-TFTs). The method successfully achieved mass transfer and bonding of Micro-LEDs with a size of $30 \times 15 \ \mu m^2$ at low temperature (180 °C) and low pressure (0.08 MPa).

1. Introduction

In the digital era, there is an increasing need for displays that have high resolution,[1] high brightness,[1b–e,2] and high color[1b–e,2] saturation. Micro light-emitting diode (Micro-LED) technology holds significant potential in several industries such as mobile phones,[3] Televisaions,[4] gaming,[5] medical equipment,[6] and military equipment.[7] It provides superior benefits such as amplified luminosity, heightened contrast, superior resolution, advanced durability, and optimized power efficiency. Micro-LED display devices consist of two major components: Micro-LED arrays and driver backplanes.[8] Micro-LED arrays are produced using a precise technique of epitaxial growth and etching on a sapphire substrate. To construct a Micro-LED display, it is typically important to establish electrical connections between millions of Micro-LED chips and the pads of the driver circuit using flip-chip bonding technology. Hence, the effectiveness and expense of Micro-LED chip transfer and bonding technology have a direct impact on the commercialization of Micro-LED display technology.

Regarding mass transfer, the initial stage in all mass transfer methods is the laser lift-off (LLO) of Micro-LED chips from sapphire substrates, as the preparation of these chips is done on such substrates.[9] Micro-LED mass transfer technology after LLO is a key obstacle limiting the popularity of the commercialization of Micro-LED display technology. Consequently, numerous investigations have been conducted, including electrostatic transfer,[10] fluidic

T. Lang, X. Lin, X. Huang, Y. Xie, S. Bai, Y. Zhou, S. Wang, Y. Lu, X. Tang, K. Zhang, Q. Yan, J. Sun
Fujian Science and Technology Innovation Laboratory for Optoelectronic Information of China, and College of Physics and Information Engineering
Fuzhou University
Fuzhou 350100, China
E-mail: jie.sun@fzu.edu.cn

C. Lin, Z. Huang
Fujian Science & Technology Innovation Laboratory for Optoelectronic Information of China
Fuzhou 350100, China

J. Sun
Quantum Device Physics Laboratory
Department of Microtechnology and Nanoscience
Chalmers University of Technology
Gothenburg 41296, Sweden

self-assembly,[11] laser transfer,[12] and stamp transfer (Indicators of these technical routes are compared in Table S1, Supporting Information).[13] While electrostatic transfer is generally steady, a high static charge might potentially harm the LED chip and result in pixel failure. Fluid self-assembly is considered a cost-effective and efficient method for transferring Micro-LEDs. However, its widespread use is hindered by the drawbacks of low transfer accuracy and a challenging repair process. At present, laser transfer and stamp transfer are the two standard processes used for the mass transfer and bonding of Micro-LEDs. The laser transfer technique offers exceptional transfer precision, rapid transfer speed, and flexible operation, enabling the efficient rearrangement of Micro-LED chips with any desired pitch. A team of researchers has successfully achieved the most minimal transfer displacement ($<0.5~\mu m$)[14] to date by utilizing laser transfer technology. This accomplishment underscores the distinct benefits of laser transfer technology in enhancing the precision of transferring Micron-sized chips. Nevertheless, laser transfer is limited to the arrangement of Micro-LED chips on a viscoelastic substrate, and thus poses challenges when attempting to connect Micro-LED chips directly to metal bumps on driver circuits that do not possess viscoelastic properties. While the transfer effectiveness of stamp transfer technology is inferior compared to laser transfer technology, it excels in achieving the bonding between the Micro-LED chip and the driver circuit. It is easy to operate and is suitable for transferring and bonding large-area chips. This technology can relocate either a single Micro-LED chip or a portion of a Micro-LED to various types of substrates.[15] Nevertheless, there are several limitations associated with the stamp transfer method. Firstly, the chip that is being transferred must be prepared on a tether structure.[13c] Additionally, the size of the chip used for the transfer must match the size of the stamp post, and the chip pitch must be a multiple of the stamp post pitch. These limits restrict the extent to which seal transfer can be applied, resulting in higher costs and decreased efficiency.

Flip chip bonding[8a,16] technique is a dependable method used in bonding technology to integrate the chip and drive substrate. Two commonly employed techniques for bonding are anisotropic conductive film (ACF) bonding[8a,17] and metal bump bonding.[16a,18] While the ACF bonding technique is simple to apply and does not require high bit precision, it is negatively impacted by the thermosetting resin in the bonded material. This makes repairing damaged pixels challenging and results in poor thermal performance of the device.[19] In contrast, the bump bonding technology utilizes individual metal bumps to establish electrical connections for Micro-LED chips. This technology enables the repair of defective pixels, provides efficient heat dissipation, and offers superior conductivity compared to ACF bonding. Commonly used metals for metal bumps include gold,[20] tin-silver,[21] tin,[22] and indium.[16a] Among them, indium has the lowest melting point of 156 °C and excellent low-temperature stability, thermal conductivity, and electrical conductivity, making it an ideal candidate for bonding Micro-LED flip-chips. However, the present transparent low-temperature polycrystalline silicon thin-film transistor (LTPS-TFT) driver substrate technique causes a height discrepancy between the substrate and the electrode due to structural design variations between the transparent area and the electrode bottom layer. The disparity in height causes an irregular thickness of the photoresist during lithography, resulting in non-uniform lithography outcomes and hindering the creation of consistent and suitably high indium bump arrays.
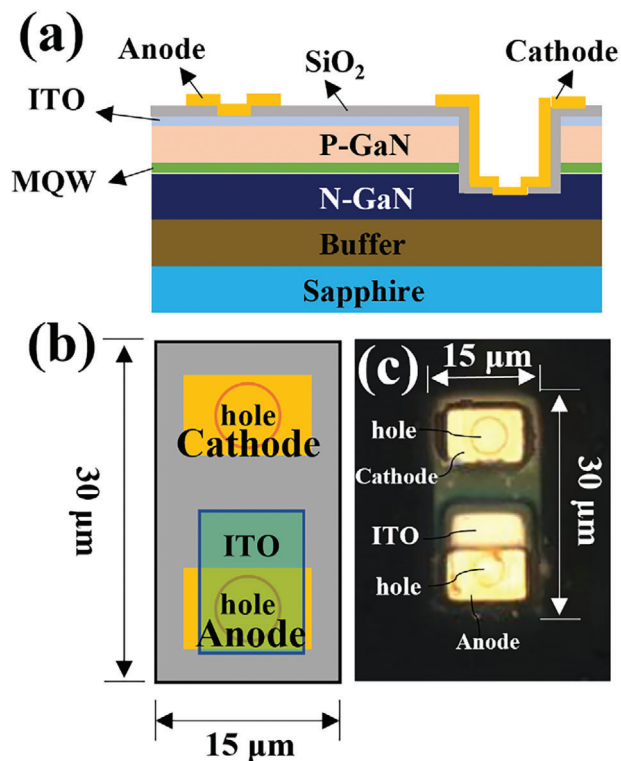
To solve the mentioned issues, we have created a technique called thin-film-assisted laser transfer and bonding (TFA-LTAB). This technique combines laser transfer with thin-film bonding, allowing for a flexible arrangement and high transfer efficiency. It eliminates the need for traditional stamp bonding that relies on tethered structures, avoids the limitations of fixed-pitch transfers, and ultimately reduces costs while improving transfer efficiency. The light-responsive film 1 was utilized for carrying out the LLO process on the Micro-LED chips, which were placed on the sapphire substrate. Afterward, a laser was used to transfer Micro-LED chips from film 1 to film 2 with a precise pitch to rearrange the Micro-LED chips. Using the laser transfer procedure, we effectively organized flip chips measuring $30 \times 15~\mu m^2$ into an 80×80 arrangement on film 2. The double-layer photoresist technique was employed to generate a suitably high photolithographic pattern on the LTPS-TFT electrode, while the uniform indium bump array was formed through evaporation. The Micro-LED display, measuring 1.98 inches, was illuminated by connecting the flip chip to the LTPS-TFT using indium bumps. This was achieved by applying a thin film 2 at a low temperature of 180 °C and low pressure of 0.08 MPa. The TFA-LTAB approach is highly suitable for large-scale production and holds promise for the commercialization of Micro-LED display technology.

2. Results and Discussion

The μ-LEDs are prepared on sapphire. The LTPS-TFT backplanes are on glass substrates. The schematic cross-sectional view of the flip chip Micro-LED, the optical image of cathode and anode electrodes designed for Micro-LED bonding, and the optical image of the fabricated backplane pixel are shown in **Figure 1a–c**, respectively. In this paper, the LED chip size is $30 \times 15~\mu m^2$.

2.1. Chip Transfer

A two-fold laser transfer method was used to prepare chip-on-carrier (COC) bonded to LTPS-TFT driver substrates. During chip-on-wafer (COW) preparation, the Micro-LED chips were tightly aligned for optimal COW utilization, as shown in **Figure 2a**, where we used a 4-inch commercially available COW. As a result, the electrode spacing on the LTPS-TFT driver substrate design did not match the spacing of the chips on the COW, which needed to be adjusted by laser. Before the first laser step, the COW was bonded to the photoresponsive film 1 (LAP811) through the bonding equipment. Due to the pressure head size limitation of our bonding equipment to $3 \times 3~cm^2$, we were not able to achieve a direct bonding of the 4-inch COW to the film 1. Therefore, we cut the COW into small pieces for bonding. Subsequently, the sapphire substrate was laser stripped, leaving the chip array on LAP811 with the electrodes facing downward, as shown in Figure 2b. Since the COW is bonded to film 1, there is no displacement in stage 1 of the transfer, and the transfer yield

**ADVANCED
SCIENCE NEWS**

www.advancedsciencenews.com

**ADVANCED
ELECTRONIC
MATERIALS**
Open Access

www.advelectronicmat.de

Figure 1. Schematic cross-section of flip chip LED structure a) with the top view b) and optical image of Micro-LEDs (c) with a chip size of 30 × 15 µm².

could reach 99.99% (see more details in Section S8 and Table S2, Supporting Information). Among other things, the inconsistent brightness of the n-type gallium nitride (GaN) surface of the chip is due to the generation of residual gallium. The second laser step is used to irradiate the light-responsive film 1. Since the film 1 is an ablative-type material that decomposes when subjected to laser irradiation, transfer of the chip is achieved by irradiating the film 1 with a laser spot at a designated location (see more details in Section S2 and Figure S1, Supporting Information). The chips were arranged on film 2 (TAP7510) according to the electrode pitch of the LTPS-TFT driver substrate, with the electrodes of the chips facing up. The results are shown in Figure 2c, where 6400 chips were displaced by less than 1 µm, and the transfer yield after repair can reach 100% in stage 2 (see more details in Section S3 and Figure S2, Supporting Information). In addition, the process of transferring from film 1 to film 2 brings polymer from the decomposition of film 1, and the removal of polymer can be achieved after we clean it (see more details in Section S4 and Figure S3, Supporting Information). In order to verify whether the transfer process causes any damage to the chip, we measured the I–V characteristics of the chip before and after LLO, and the results are shown in Figure 2d, which indicates that there is no obvious electrical damage.

2.2. Driving Substrate Bump Preparation

The procedures involved in bump fabrication are delineated in **Figure 3a–f**. The photolithography involves the utilization of a double-layer photoresist for patterning. The primary layer is to minimize the height disparity and enhance the substrate's planarity. The specific pattern is established via the application of the second photoresist layer. The outcomes derived from photolithography are graphically depicted in Figure 3a,b. Importantly, the choice of materials for the first and second photoresists is strategic, opting for those with maximum similarity. This is to bypass the possibility of non-uniform film layer issues, which may result from discrepancies in wettability during the spin-coating process of the second layer. In order to resolve potential issues that may arise due to the presence of residual photoresist in the pattern, which could disrupt metal deposition prior to vacuum thermal evaporation deposition, a procedure employing oxygen plasma treatment for a duration of ≈3 min is executed prior to metal deposition. This crucial step aids in eliminating any residual photoresist while also augmenting the surface wettability of the sample, a key factor that further facilitates the enhancement of metal adhesion. Gold was deposited on the TFT electrode using vacuum thermal evaporation for under-bump metallurgy, followed by the deposition of indium bumps using the same method. The experimental results, as depicted in Figure 2c, reveal complete concave holes on the surface without any blockage by the deposited material. After removing the photoresist, the array of In bumps adhering to the electrodes without being altered is presented in Figure 3d. Figure 3e displays the outcomes of a detailed scanning electron microscopy (SEM) study conducted at high magnification. The irregularity of the bump surface is caused by the varying rate of indium evaporation as the mass of indium in the evaporation boat diminishes. The focused ion beam (FIB) examination of a single bump is shown in Figure 3f, revealing a high concentration of indium within the bump. Figure S6 (Supporting Information) demonstrates that the height of the bumps possesses good uniformity.

2.3. Bonding

A high-precision transfer bonding machine facilitated the bonding process between COC and prepared TFT bumps. This equipment supports simultaneous heating treatment of both COC and TFT, providing precise control over the bonding temperature. It allows for variable rates of separation, which is a critical factor in managing the viscosity of viscoelastic materials. Adjusting the separation rate effectively isolated the Micro-LED from the colloid, ensuring proper soldering onto the TFT bump. The LTPS-TFT substrate was heated to 130 °C, closely approaching but not reaching the indium melting point, to maintain stable indium morphology while simultaneously preparing it for subsequent low-pressure bonding. COC was heated to 180 °C to gently melt the Micro-LED upon contact with the TFT bump. After the COC was precisely aligned with the LTPS-TFT, low-pressure bonding was performed at a pressure of 0.08 MPa (the area over which the pressure is calculated is the area of the TAP, considering that the TAP is an elastic material and the entire face touches the substrate when pressure is applied). Upon completion of the bonding process, COC cooling induces solidification of the indium bumps, which are then subjected to controlled separation, enabling efficient Micro-LED soldering on LTPS-TFTs.
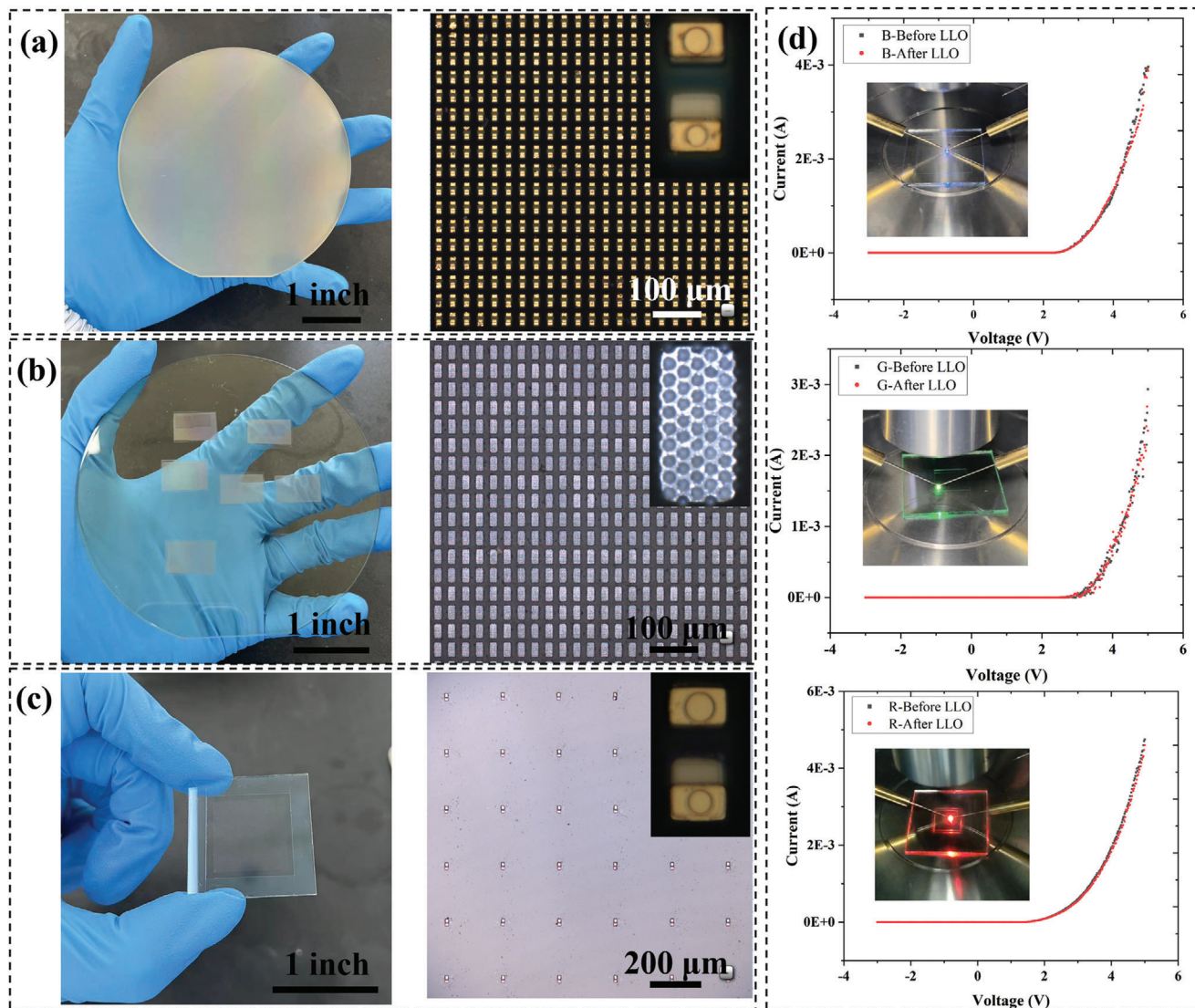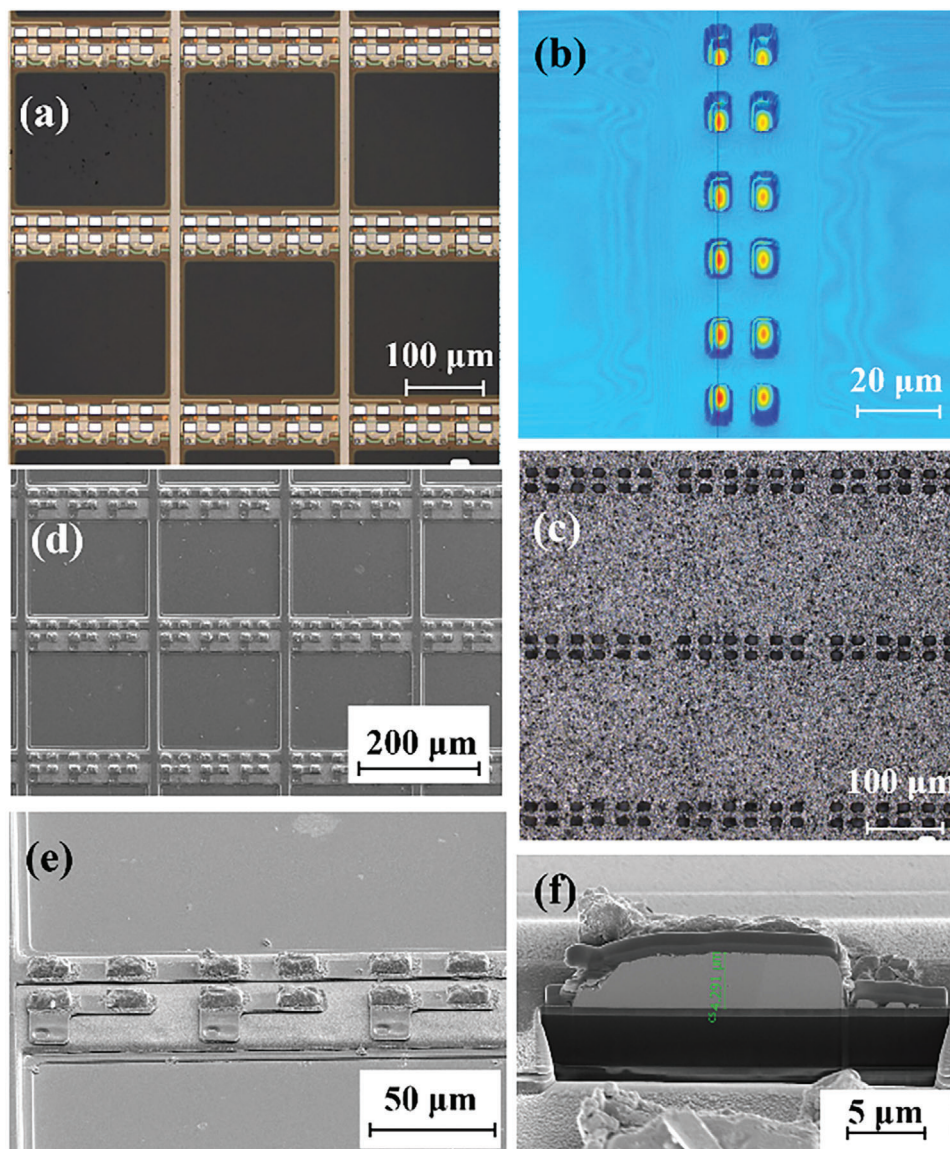
Figure 2. Chip transfer process. a) The image on the left shows a Micro-LED array fabricated on a 4-inch sapphire substrate. The image on the right shows a portion of the Micro-LED array at higher magnification. b) The image on the left shows the Micro-LED array left on film 1 after the LLO process, and the image on the right shows a portion of the array at higher magnification. c) The left image demonstrates further transfer of the Micro-LED array onto film 2 and lined up at a specific pitch. The right figure demonstrates a better magnification image of the same array. d) Shows the *I–V* characteristics of Micro-LEDs before and after the transfer of three colors of RGB.

After completing the bonding process, COC cooling induced indium bump solidification, followed by a controlled separation to achieve effective Micro-LED soldering on LTPS-TFTs. Low- and high-magnification images of successfully bonded areas on the LTPS-TFT are presented in **Figure 4a,b**. To address the potential for indium bump oxidation during bonding, a controlled nitrogen atmosphere was introduced throughout the process to mitigate further oxidation. After several bonding experiments, a detailed analysis of the indium bumps on LTPS-TFTs was conducted by cutting a single indium bump using FIB and performing a cross-section analysis, as depicted in Figure 4c. The findings revealed a thin oxide layer, ≈20.5 nm thick, on the indium bump surface. Energy Dispersive Spectrometer (EDS) analysis is shown in Figure 4d, indicated that indium constituted ≈50% of the gravity, with oxygen accounting for ≈8%, suggesting a low degree of oxidation in the bumps. Finally, **Figure 5a–d** illustrates the illumination effect of a Micro-LED achieved through successful bonding and merging. In Figure 5a,b, red Micro-LEDs are illuminated using probes and circuits, respectively, with images captured through microscopic observation. Figure 5c shows the illumination effect of green Micro-LEDs, while Figure 5d,e display the illumination effect of blue Micro-LEDs with different areas. The final bonding yield of our 1.98-inch Micro LED display was ≈80%. There are a number of factors that can affect bonding yields, such as bond force, indium bump height uniformity, regularity of bump surface topography, bonding temperature and bonding time, etc., and we have summarized the results that can occur under different bonding conditions (see more details in Section S3 and Figure S2, Supporting Information). Although there are various factors that affect the process and lead to a

2400380 (4 of 8)

**ADVANCED
SCIENCE NEWS**

www.advancedsciencenews.com

**ADVANCED
ELECTRONIC
MATERIALS**

www.advelectronicmat.de

Figure 3. Indium bump preparation process. a) 2D optical images and b) 3D images lithographed with bilayer photoresists, c) thermal evaporation deposition of gold and indium metal films. d) SEM images of the indium bump array on TFT electrodes, e) the higher magnification SEM image of the indium bumps array, and f) a cross-section image of a single bump.

reduction in the final yield, the focus of our subsequent work will be to optimize the above conditions to achieve higher bonding yields.
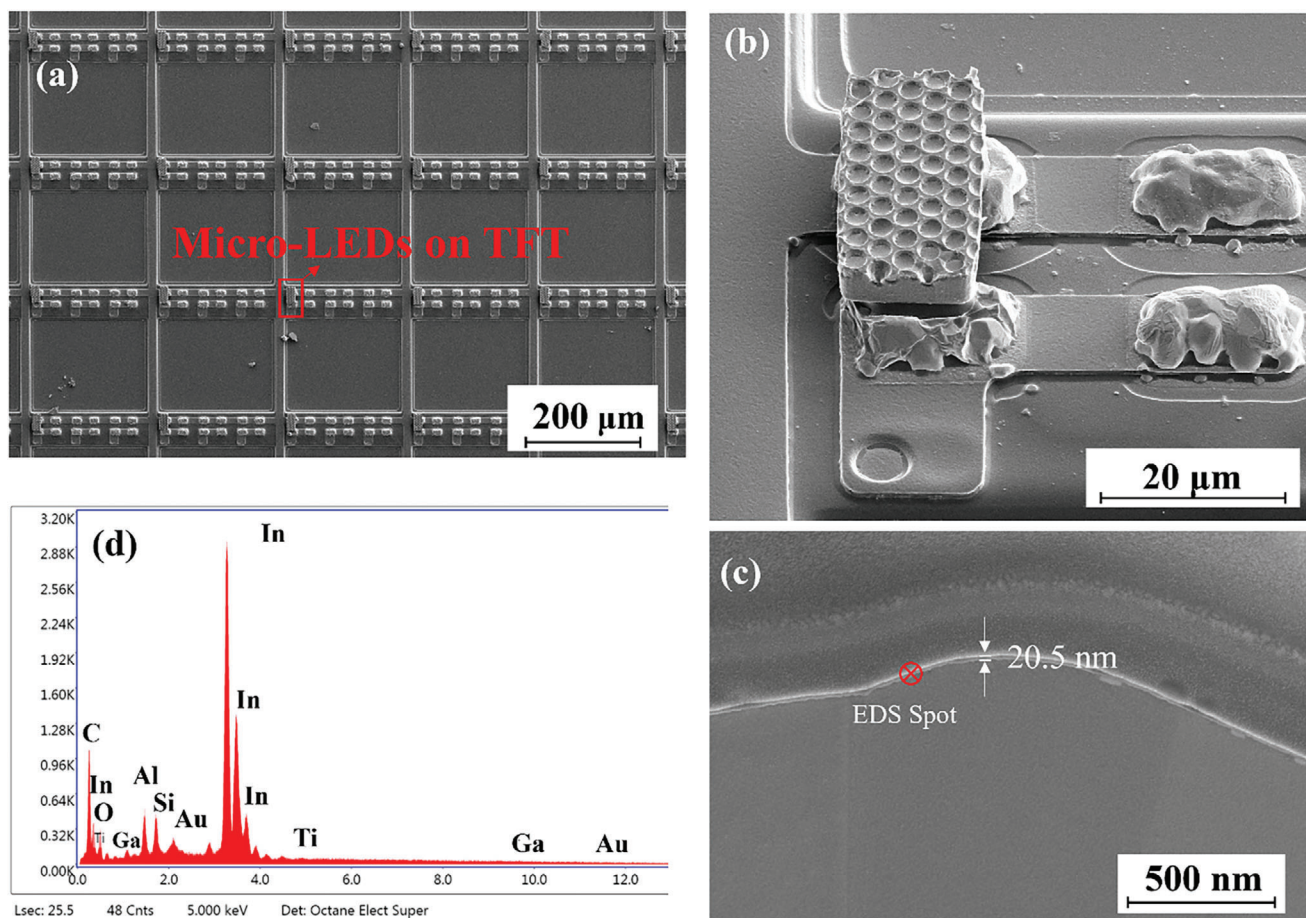
3. Conclusion

With TFA-LTAB technology, our team has made significant progress in the field of display technology. We successfully transferred chips from the sapphire substrate to LTPS-TFT and realized its illumination function, which marks a key breakthrough in AMLED display technology. Using precise low-temperature, low-pressure bonding technology, we achieved the precise transfer of red (R), green (G), and blue (B) chips, where the pixel size was controlled at $30 \times 15 \ \mu m^2$ and the pixel pitch was maintained at 222 Microns. Our AMLED display shows excellent color per-formance in all three colors, R, G, and B. Our proposed method of using TFA-LTAB is one that holds greater promise for application because the thin film is made by a spin-coating process, which is now mature enough to be applicable to most scenarios, such as large-area transfers.This not only validates the effectiveness of our technical solution but also provides a clear development roadmap for the future development of full-color AMOLED displays and the overall advancement of display technology.

4. Experimental Section

Materials: LTPS-TFT was obtained from Tianma Microelectronics Co., Ltd. COW was purchased from Xiamen Changelight Co., Ltd. LAP811

ADVANCED
SCIENCE NEWS

www.advancedsciencenews.com

ADVANCED
ELECTRONIC
MATERIALS

www.advelectronicmat.de

Figure 4. Chip bonding results. a) SEM image of the chip successfully bonded to the TFT and b) high magnification image, c) cross-section of the bump after multiple bonding, d) EDS analysis results of the oxide layer.

and TAP7510 were obtained from Samcien Semiconductor Materials Co., Ltd.

Methods—COC Preparation: A twofold laser transfer technique was used to transfer the chip from the sapphire substrate to film 2 (TAP7510) at the same pitch as the driver substrate. The details of the experiments were as follows: after spin-coating film 1 (LAP811) on carrier 1 and curing at 100 °C for 5 min, the COW was cut into small pieces and bonded to film 1, and then the sapphire substrate was removed using the first laser, a process which yielded the transfer of the chip arrays to film 1. Subsequently, film 2 (TAP7510) was spin-coated on carrier 2, and after curing at 160 °C for 5 min, the chips were again transferred to film 2 using a second laser at the target spacing to obtain the COC, (schematic shown in Figure S4, Supporting Information).

Methods—Driver Substrate Bump Preparation: Since the driver substrate was fabricated with most of the area of the organic layer removed in order to improve transparency, it resulted in a 7 µm height difference between the electrodes and the bottom layer of the driver substrate. Usually, a thick photoresist can be used to achieve lithography, but the height difference causes inconsistency of the thick photoresist at different heights under the same lithography conditions. Therefore, a two-layer photoresist approach was developed to achieve bump patterning, in which the first layer of photoresist uses a photoresist (AZ 2070) of ≈7 µm to fill the height difference of the substrate, and the second layer uses the same photoresist (which reduces

the effect of the difference in wettability caused by the inconsistency of the material) to perform the normal process of photolithography. Subsequently, vacuum thermal evaporation is used for the deposition of Au and In, and finally the photoresist is removed to obtain the bump array, as shown schematically in Figure S5 (Supporting Information).

Methods—Bonding of COC to Driver Substrate: The COC was bonded to the TFT using a micron chip transfer machine FC3000MSF. In the bonding process, the COC was heated to 180 °C and the driver substrate was heated to 130 °C, and the bonding was carried out by precise alignment using a pressure of 0.08 MPa, followed by cooling down to room temperature and separating the film 2. The chip array was then electrically connected to the driver substrate. The process is shown schematically in Figure S7 (Supporting Information).

Characterization: An optical microscope was employed for initial observations, followed by the utilization of a 3D measurement laser microscope (LEXT OLS4100) to obtain precise data and topological information about the process. Additionally, SEM and FIB-assisted scanning electron microscopy (FIB; Helios G4CX) were used to enhance the understanding of the results, specifically to observe the characterization of the chip bonded to the bumps and the bump cross-section morphology. The integration of these multiple characterization methods serves to complement each other, providing comprehensive and detailed process information essential for the optimization and improvement of the study.

(First revision and second revision mark.)
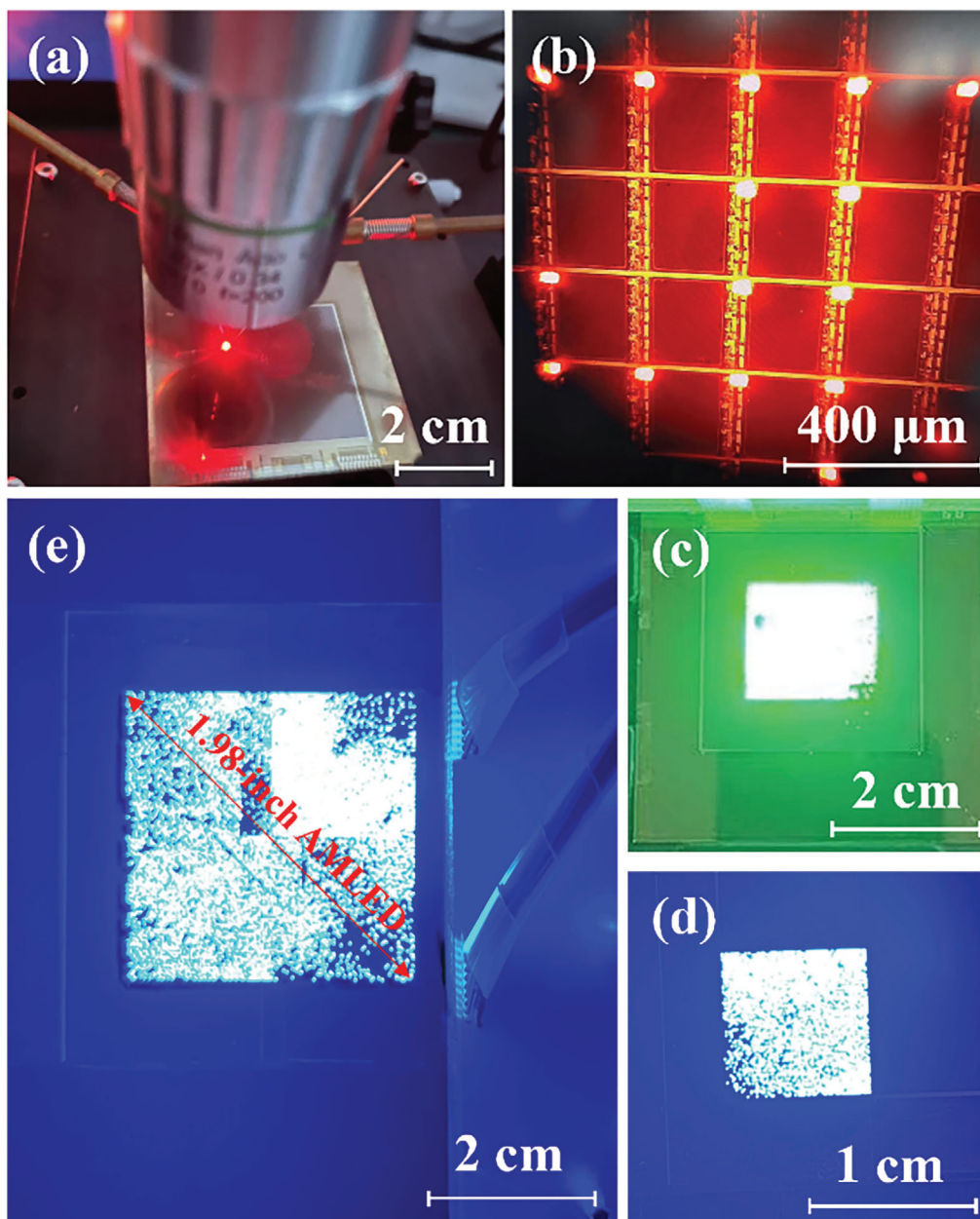
Figure 5. R/G/B chip lighting pictures. a) Photographs of the probe lighting a single chip as well as b) Microscope pictures of large area lighting, c) green Micro-LED, d) blue Micro-LED, and e) 1.98-inch blue Micro-LED.

Supporting Information

Supporting Information is available from the Wiley Online Library or from the author.

Conflict of Interest

The authors declare no conflict of interest.

Data Availability Statement

The data that support the findings of this study are available from the corresponding author upon reasonable request.

[1] a) H. X. Jiang, S. X. Jin, J. Li, J. Shakya, J. Y. Lin, *Appl. Phys. Lett.* **2001**, *78*, 1303; b) M. S. Wong, S. Nakamura, S. P. DenBaars, *ECS J. Solid State Sci. Technol.* **2019**, *9*, 015012; c) T. Wu, C.-W. Sher, Y. Lin, C.-F. Lee, S. Liang, Y. Lu, S.-W. Huang Chen, W. Guo, H.-C. Kuo, Z. Chen, *Appl. Sci.* **2018**, *8*, 1557; d) G. Biwa, A. Aoyagi, M. Doi, K. Tomoda, A. Yasuda, H. Kadota, *J. Soc. Inf. Disp.* **2021**, *29*, 435; e) H. X. Jiang, J. Y. Lin, *Opt. Express* **2013**, *21*, A475.

[2] a) W. C. Chong, W. K. Cho, Z. J. Liu, C. H. Wang, K. M. Lau, presented at Compound Semiconductor Integrated Circuit Symposium, IEEE, La Jolla, CA, USA, October, **2014**; b) R.-H. Horng, H.-Y. Chien, F.-G. Tarntair, D.-S. Wuu, *IEEE J. Electron Devices Soc.* **2018**, *6*, 1064; c) K. Zhang, D. Peng, K. M. Lau, Z. Liu, *J. Soc. Inf. Disp.* **2017**, *25*, 240; d) L. Zhao Jun, W. Ka Ming, K. Chi Wing, T. Chak Wah, L. Kei May, *IEEE J. Sel. Top. Quantum Electron.* **2009**, *15*, 1298.

[3] a) C.-H. Chu, *Multimedia Systems* **2012**, *19*, 315; b) J. Kimmel, J. Hautanen, T. Levola, *Proceedings of the IEEE* **2002**, *90*, 581.

[4] a) Y. Ishii, *J. Disp. Technol.* **2007**, *3*, 351; b) M. Nishikawa, *J. Photopolym. Sci. Technol.* **2011**, *24*, 317.

[5] a) A. Hogue, B. Kapralos, C. Zerebecki, M. Tawadrous, B. Stanfield, U. Hogue, *Stereoscopic 3D video games and their effects on engagement*, Vol. 8288, SPIE **2012**; b) S.-J. Chen, Y.-Y. Kang, C.-L. Lin, *J. Ambient Intell. Humaniz. Comput.* **2016**, *7*, 845.

[6] C. Lovis, A. Yamazaki, P. Liu, W.-C. Cheng, A. Badano, *PLoS One* **2013**, *8*.

[7] M. Bayer, *Retinal scanning display: a novel HMD approach for Army aviation*, Vol. 4711, SPIE **2002**.

[8] a) J. G. Um, D. Y. Jeong, Y. Jung, J. K. Moon, Y. H. Jung, S. Kim, S. H. Kim, J. S. Lee, J. Jang, *Adv. Electron. Mater.* **2018**, *5*, 1800617; b) Z. Gong, E. Gu, S. R. Jin, D. Massoubre, B. Guilhabert, H. X. Zhang, M. D. Dawson, V. Poher, G. T. Kennedy, P. M. W. French, M. A. A. Neil, *J. Phys. D: Appl. Phys.* **2008**, *41*, 094002; c) J. J. D. McKendry, R. P. Green, A. E. Kelly, Z. Gong, B. Guilhabert, D. Massoubre, E. Gu, M. D. Dawson, *IEEE Photonics Technol. Lett.* **2010**, *22*, 1346; d) B. R. Rae, C. Griffin, J. McKendry, J. M. Girkin, H. X. Zhang, E. Gu, D. Renshaw, E. Charbon, M. D. Dawson, R. K. Henderson, *J. Phys. D: Appl. Phys.* **2008**, *41*, 094011.

[9] F. Chen, J. Bian, J. Hu, N. Sun, B. Yang, H. Ling, H. Yu, K. Wang, M. Gai, Y. Ma, Y. Huang, *Int. J. Extrem. Manuf.* **2022**, *4*, 042005.

[10] a) L. B. Biedermann, T. E. Beechem, A. J. Ross, T. Ohta, S. W. Howell, *New J. Phys.* **2010**, *12*, 125016; b) S. Kim, Y. Jiang, K. L. Thompson Towell, M. S. H. Boutilier, N. Nayakanti, C. Cao, C. Chen, C. Jacob, H. Zhao, K. T. Turner, A. J. Hart, *Sci. Adv.* **2019**, *5*, 4790.

[11] a) H.-J. J. Yeh, J. S. Smith, *IEEE Photonics Technol. Lett* **1994**, *6*, 706; b) W. Chang, J. Kim, M. Kim, M. W. Lee, C. H. Lim, G. Kim, S. Hwang, J. Chang, Y. H. Min, K. Jeon, S. Kim, Y.-H. Choi, J. S. Lee, *Nature* **2023**, *617*, 287.

[12] a) H. Luo, S. Wang, C. Wang, C. Linghu, J. Song, *Adv. Funct. Mater.* **2021**, *31*, 2010297; b) K. S. Kaur, J. Missinne, G. Van Steenberge, *Appl. Phys. Lett.* **2014**, *104*, 061102; c) C. K. W. Lee, Y. Pan, R. Yang, M. Kim, M. G. Li, *Top. Curr. Chem.* **2023**, *381*, 18.

[13] a) K. Glasmästar, J. Gold, A. S. Andersson, D. S. Sutherland, B. Kasemo, *Langmuir* **2003**, *19*, 5475; b) M. A. Meitl, Z.-T. Zhu, V. Kumar, K. J. Lee, X. Feng, Y. Y. Huang, I. Adesida, R. G. Nuzzo, J. A. Rogers, *Nat. Mater.* **2006**, *5*, 33; c) R. S. Cok, M. Meitl, R. Rotzoll, G. Melnik, A. Fecioru, A. J. Trindade, B. Raymond, S. Bonafede, D. Gomez, T. Moore, *J. Soc. Inf. Disp.* **2017**, *25*, 589.

[14] Z. Pan, C. Guo, X. Wang, J. Liu, R. Cao, Y. Gong, J. Wang, N. Liu, Z. Chen, L. Wang, M. Ishikawa, Z. Gong, *Adv. Mater. Technol.* **2020**, *5*, 2000549.

[15] a) S.-I. Park, Y. Xiong, R.-H. Kim, P. Elvikis, M. Meitl, D.-H. Kim, J. Wu, J. Yoon, C.-J. Yu, Z. Liu, Y. Huang, K.-c. Hwang, P. Ferreira, X. Li, K. Choquette, J. A. Rogers, *Science* **2009**, *325*, 977; b) C. A. Bower, M. A. Meitl, B. Raymond, E. Radauscher, R. Cok, S. Bonafede, D. Gomez, T. Moore, C. Prevatte, B. Fisher, R. Rotzoll, G. A. Melnik, A. Fecioru, A. J. Trindade, *Photon. Res.* **2017**, *5*, A23.

[16] a) X. Ji, F. Wang, P. Lin, L. Yin, J. Zhang, *IEEE Trans. Electron Devices* **2022**, *69*, 3737; b) J. Day, J. Li, D. Y. C. Lie, C. Bradford, J. Y. Lin, H. X. Jiang, *Appl. Phys. Lett.* **2011**, *99*, 031116; c) X. Ji, F. Wang, L. Yin, J. Zhang, In *2021 18th China International Forum on Solid State Lighting & 2021 7th International Forum on Wide Bandgap Semiconductors (SSLChina: IFWS)*, Shenzhen, China **2021**.

[17] a) Y. C. Chan, D. Y. Luk, *Microelectronics Reliability* **2002**, *42*, 1195; b) K. Lee, H. J. Kim, I. l. Kim, K. W. Paik, In *2007 Electronic Components and Technology Conference*, IEEE, Piscataway, NJ, USA **2007**, *5*; c) W.-S. Kwon, K.-W. Paik, *Int. J. Adhes. Adhes.* **2004**, *24*, 135; d) K. H. Ryu, N. Kwon, M. H. Seo, M. H. Lee, G. J. Nam, N. H. Kwak, *IEEE Trans. Adv. Packag.* **2006**, *29*, 701.

[18] a) W. Fu, M. Nimura, T. Kasahara, H. Mimatsu, A. Okada, S. Shoji, S. Ishizuka, J. Mizuno, *J. Electron. Mater.* **2015**, *44*, 4646; b) F. Greer, M. Dickie, R. P. Vasquez, T. J. Jones, M. E. Hoenk, S. Nikzad, *Meas., Phenom.* **2009**, *27*, 2132; c) Z. Jianhua, W. Changhai, Z. Jun, P. Ah Ju, *IEEE Trans. Compon. Packag. Technol.* **2007**, *30*, 781; d) N. Watanabe, Y. Ootani, T. Asano, *Jpn. J. Appl. Phys.* **2005**, *44*, 2751.

[19] a) J. Joo, C. Lee, I. S. Kye, Y. S. Eom, K. S. Jang, G. M. Choi, S. H. Moon, H. G. Yun, K. S. Choi, presented at *IEEE Electronic Components and Technology Conference*, San Diego, CA, USA August, **2021**; b) K. S. Choi, *Etri Journal* **2011**, *33*, 637; c) K.-S. Choi, Y.-S. Eom, S. H. Moon, J. Joo, l. Jeong, K. Lee, J. H. Kim, J. h. Kim, G.-S. Yoon, K.-H. Lee, C.-H. Lee, G.-S. Ahn, M.-S. Shim, In *2019 IEEE 69th Electronic Components and Technology Conference (ECTC)*, IEEE, Las Vegas, Nevada, USA, **2019**, *5*; d) Y. S. Eom, K. S. Jang, J. T. Moon, J. D. Nam, *ETRI Journal* **2010**, *32*, 414.

[20] J. H. Kim, B. C. Kim, J. Lee, C. D. Yoo, *Sci. Technol. Weld. Joining* **2005**, *10*, 604.

[21] B. Neveu, F. Lallemand, G. Poupon, Z. Mekhalif, *Appl. Surf. Sci.* **2006**, *252*, 3561.

[22] Z. Hu, C. Liou, C. Tsou, *IEEE Trans. Compon., Packag., Manuf. Technol.* **2023**, *13*, 2040.